Simulation of Traveling Wave Toner Transport

Ralph Kober
Technical Electronics Institute, Aachen University of Technology
Aachen, Germany

Abstract

A numerical computation of the dynamic flow of charged toner particles on a traveling electrostatic wave device is presented. In contrast to simple single particle models, the simulation is performed for a large ensemble of toner particles and takes into account mechanical and electrical interactions. This more realistic computation is based on a two-dimensional finite element field calculation of the imposed traveling electrostatic wave. The particles are modeled as spheres of different sizes, each carrying a point charge inside. Boundary conditions at the substrate surface are met by the method of image charges. Collective electrostatic effects that tend to force the particles towards the conveyor surface are described by an additional electric field accounting for the space charge in the toner cloud. Besides the mutual electrical interactions, collisions between the particles and impact forces at the conveyor surface are included in the calculations as well. Simulations with an ensemble of 250 particles are shown and discussed relative to experimental results.

1. Introduction

Traveling wave devices create running electrostatic waves along their boundary which are capable of transporting charged powders in a controlled fashion. Because of their ability to transport dry toner particles without moving parts they may be an advantageous technology for xerographic and electrostatic printers.[1,2] But so far, most of the theoretical work in the field of traveling wave toner transport has focused on the motion of a single particle.[2-10] With numerical calculations using such a simple model it is not possible to study the effects of particle interaction which are certainly present in realistic applications. This problem has been discussed by Gartstein, Shaw, Thompson and LeStrange.[11,12] They were the first to publish simulations based on a many-particle model. Their calculations were done with a 3-dimensional particle-in-cell computer model.[13,14] In this paper many-particle simulations with a new 2-dimensional model are presented and compared with experimental results.

2 Description of the Model

During the simulation the movement of an ensemble of charged toner particles is calculated by simultaneously solving their equations of motion. The model takes into account mechanical forces due to inertia, air drag (Stoke's law), friction, gravity, collisions between particles and collisions between particles and the conveyor surface. Origins of electrical forces are the electric field imposed by the conveyor electrodes and mutual interactions between the charged toner particles.

2.1 Equations of Motion

In this model the particles are allowed to move only in two dimensions. With the coordinates being (x; z) the equations of motion are

$$m \bullet \frac{d^2x}{dt^2} + 6\pi\eta a \frac{dx}{dt} = qE_x + F_{fric} \tag{1}$$

$$\underbrace{m \bullet \frac{d^2z}{dt^2}}_{Inertia} + \underbrace{6\pi\eta a \frac{dz}{dt}}_{Stoke's\ drag} = \underbrace{qE_z - mg}_{F_z, F_z} \tag{2}$$

where

m : particle mass;
q : particle charge;
a : particle radius;
η : viscosity of air;
g : gravitational acceleration;
$E = (E_x; E_z)$: electric field strength

The friction force F_{fric} is applied only if the particle is in contact with the conveyor surface ($z = a$) and the normal force F_z is pointing toward the grid surface ($F_z < 0$). If one or both conditions are not satisfied F_{fric} is zero.

2.2 Friction

Friction can be either static or dynamic, depending on the particle velocity v_x. It is characterized by the corresponding coefficients of friction, here labeled μ_s and μ_d. In this paper the coefficients are taken as $\mu_s = 1.0$ and $\mu_d = 0.4$.

In the case of $v_x = 0$ the static friction force is

$$F_{fric,stat} = \begin{cases} -qE_x & \text{if } |qE_x| \le \mu_s |F_z| \\ -sign(qE_x) \cdot \mu_s |F_z| & \text{if } |qE_x| \le \mu_s |F_z| \end{cases} \tag{3}$$

while the dynamic friction force ($v_x \neq 0$) is

$$F_{fric,dyn} = -\text{sign}(v_x) \cdot \min\left\{\mu_d |F_z|, |F_{stop}|\right\} \tag{4}$$

The term F_{stop} describes the particular force that would have to be applied to stop the motion of the particle during the next iteration step Δt. It is a natural limit which must not be exceeded, otherwise the particle would start to move in the opposite direction, even if its velocity would normally drop to zero. For example, when using a simple Euler method the particle will oscillate instead of coming to rest. With the more robust fourth-order Runge-Kutta technique,[15] which is used in this model, the particle will end up sliding at a very low speed even if no electrical forces are applied.

Unfortunately, due to the multiple extrapolation steps within the Runge-Kutta algorithm, the force F_{stop} cannot be calculated straightforward. It would have to be done iteratively. A more simple technique is to calculate the force limit for an Euler step and use it as an approximation in the Runge-Kutta algorithm. Then, the particle does not stop immediately, but its velocity v_x typically decreases several orders of magnitude per iteration and the particle will stop very soon. When applying this technique, the friction force limit is

$$F_{stop} = v_x\left(6\pi\eta a - \frac{m}{\Delta t}\right) - qE_x \tag{5}$$

which can be derived from the condition for the mentioned Euler step

$$v_x + \frac{dv_x}{dt}\cdot\Delta t = 0 \tag{6}$$

2.3 Electric Field

Two components contribute to the electrical forces experienced by a particle: the electric field imposed by the conveyor electrodes and mutual interactions between the charged particles. The electric field which is generated by the electrodes is calculated semi-analytically based on a finite element analysis.

Particle interactions are included in the simulation in two complementary ways. The first is that each particle is modeled as a sphere carrying a point charge in its center. To meet the boundary conditions at the conveyor surface for each particle an image charge is introduced. The electrical force between two of the particles or images is calculated by Coulomb's law. This force has only a short range because it falls off as the inverse squared distance.

Compared to a typical application the number of toner particles in this many-particle model is still very small and in reality the collective electrostatic effects are much stronger than those of a few point charges. In general the space charge inside the traveling toner cloud creates an electrostatic field which forces the toner particles towards the conveyor surface. This space charge effect is included in the calculation through a corresponding electric field E_{space}.

Collecting all the aforementioned terms the electric field can be expressed as

$$E = \underbrace{E_{conv}}_{\text{Conveyor}} + \underbrace{E_q + E_{q,image} + E_{space}}_{\text{Particles charges}} \tag{7}$$

Herein the electric field of the conveyor electrodes is the most important part. It is calculated with the FEM software Mag-Net (Infolytica Corporation). A sectional view of the modeled device is shown in Fig. 1. It consists of stripe electrodes on a substrate and an insulating layer on top. The dimensions in the schematic are p = 635 µm and d = 60 µm. Experimental work with similar toner conveyors has been described in former papers.[16,17] In general the conveyor may have $L \geq 3$ phases, but most of the following examples will focus on a 3 phase system.

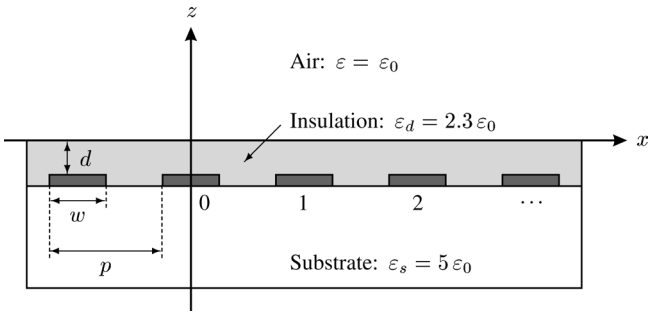

Figure 1. Sectional view of the toner conveyor

For the field calculation the superposition principle can be used which means that only the electric field of one phase needs to be determined. For example, in Fig. 2 the electrostatic potential Φ_0 in the plane $z = -d$ is plotted for the case that a voltage U_0 is applied only to the electrodes of the first phase which is named phase 0 (see Fig. 1). The other electrodes are grounded. Because the electrostatic potential is periodical with the conveyor wavelength $\lambda = L \cdot p$ and also symmetrical, the curves are just plotted for the first half period $0 \leq x \leq \lambda/2$.

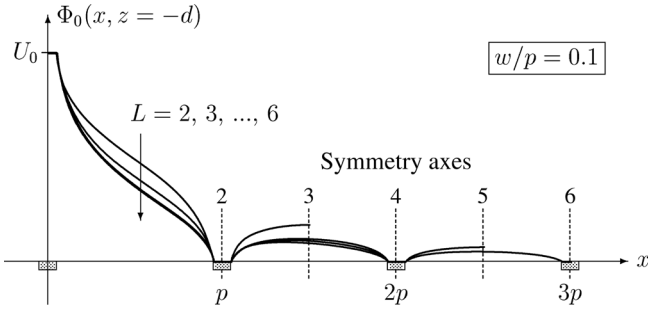

Figure 2. Electrostatic potential Φ_0 in the plane $z = -d$

In the next step the calculated periodical potential is expanded in a Fourier series of spatial frequencies:

$$\Phi_0(x, z=-d) = U_0 \cdot \sum_{n=0}^{C} a_n \cos(nkx) \tag{8}$$

In this equation $k = 2\pi/\lambda$ is the wave-number. The unknown Fourier coefficients a_n are calculated numerically

through a Discrete Fourier Transform[18] from 1024 sampling points of the curves in Fig. 2. It yields an identical number of Fourier coefficients, thus C is 1023. From solving the Laplace equation $\Delta\Phi_0 = 0$ the electric potential in the air filled halfspace $z \geq 0$ can be derived as

$$\Phi_0(x,z,t) = u_0(t) \cdot \sum_{n=0}^{C} \frac{a_n \cdot \cos(nkx) \cdot e^{-nkz}}{\cosh(nkd) + \frac{\varepsilon_d}{\varepsilon_0}\sinh(nkd)} \tag{9}$$

for the case that a voltage $u_0(t)$ is applied solely to the electrodes of phase 0.

To generate a traveling electrostatic wave suitable for toner transport, L phase shifted voltages are applied to the electrodes of the conveyor. The electric potential is found through a superposition of the time and space shifted contributions of all phases.

$$\Phi_{conv}(x,z,t) = \sum_{m=0}^{L-1} \Phi_0\left(x - m\frac{\lambda}{L}, z, t - m\frac{T}{L}\right) \tag{10}$$

An example of the resultant traveling electrostatic wave is shown in Fig. 3.

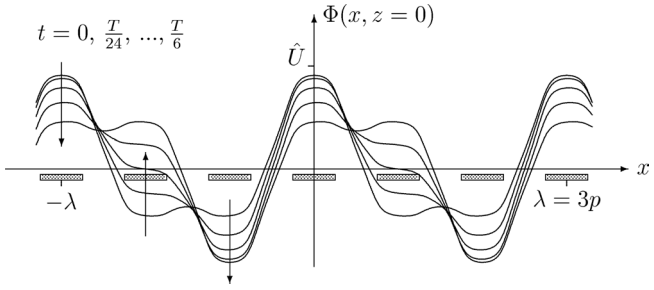

Figure 3. Traveling electrostatic wave at the surface $z = 0$. In this example sinusoidal voltages with an amplitude $\hat{U}$ and a frequency $f = 1/T$ are applied to the electrodes of the three phase conveyor.

Finally, when the motion of one of the N particles has to be calculated from Eqs. (1) and (2) the electric field must be evaluated at its position. For the i-th particle located at (x_i, z_i) the field strength is

$$E_{conv}(x_i,z_i,t) = -\nabla\Phi_{Conv}(x,z,t)\Big|_{(x_i,z_i)} \tag{11}$$

The electric field due to other particles in the model is

$$E_q(x_i,z_i) = \frac{1}{4\pi\varepsilon_0}\sum_{n\neq i}^{N} q_n \frac{r_1}{|r_1|^3} \tag{12}$$

Similarly, the field of the image charges is

$$E_{q,image}(x_i,z_i) = -\frac{1}{4\pi\varepsilon_0}\cdot\frac{\varepsilon-\varepsilon_0}{\varepsilon+\varepsilon_0}\sum_{n=i}^{N} q_n \frac{r_2}{|r_2|^3} \tag{13}$$

with the distance vectors

$$r_1 = \begin{pmatrix} x_i - x_n \\ z_i - z_n \end{pmatrix} \text{ and } r_2 = \begin{pmatrix} x_i - x_n \\ z_i + z_n \end{pmatrix} \tag{14}$$

A certain limitation of the model is that the additional space charge field E_{space} cannot be calculated exactly, so far. The actual space charge density in the traveling toner clouds is still unknown. Nevertheless, in most cases the condition $E_{space,x} \approx 0$ should apply. For simplicity, in the simulation the collective electric field is assumed as a constant field $E_{space,z}$ of moderate strength that forces the particles downwards.

2.4 Particle Collisions

An important part of the simulation is the handling of collision events. As shown in Fig. 4 these can be either particle-to-particle or particle-to-surface collisions.

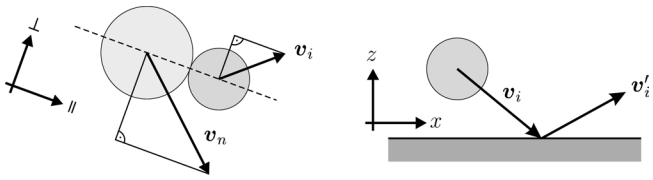

Figure 4. Particle-to-particle and particle-to-surface collision

Energy loss occurring during a collision is described by a restitution coefficient C_r that alters the velocity component which is parallel to the direction of contact. After an impact between the i-th and n-th particle their parallel velocity components are

$$v'_{\parallel,i} = v_{\parallel,i} + [1 + C_r]\frac{m_n}{m_i + m_n}\cdot(v_n - v_i) \tag{15}$$

$$v'_{\parallel,n} = v_{\parallel,n} + [1 + C_r]\frac{m_i}{m_i + m_n}\cdot(v_i - v_n) \tag{16}$$

while their perpendicular components $v_{\perp,i}$ and $v_{\perp,n}$ remain unchanged. Similar to this a particle-to-surface collision is handled as $v'_{x,i} = v_{x,i}$ and $v'_{z,i} = -C_r \cdot v_{z,i}$.

For both collision types the restitution coefficient is assumed as $C_r = 0.2$.

A challenging problem that cannot be discussed in detail in this paper is the proper detection and handling of collisions in large particle ensembles. The rather simple algorithm described by Shaw et al.[13] was found to be unsatisfactory for this model. It has the flaw that particle overlaps can accumulate during the simulation. This can lead to serious problems when computing over long times, especially if the restitution coefficient is low. Therefore, a more sophisticated algorithm has been developed which avoids particle overlaps at all.

2.5 Charge and Size Distribution

The sizes of the particles are chosen to fit the log normal distribution of an experimental toner. Figure 5 depicts that 90 volume percent of the toner particles are in a range of 12 - 23 µm with a mean diameter of approximately 14 µm.

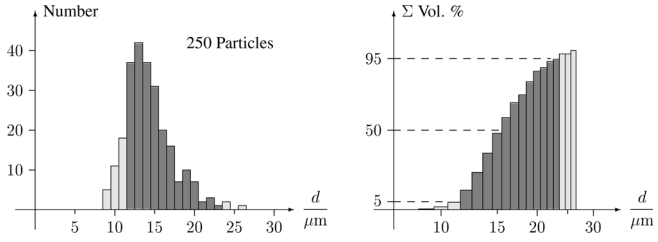

Figure 5. Particle size distribution. On the left the number of particles in a each sizeclass is shown. On the right the volume portion of all particles up to a particular diameter is displayed

The experimentally measured mean charge-to-mass ratio is q/m = 7mC/kg. Without further knowledge of the charge distribution here all particles are simply assumed to have the same charge $q = 1.7 \cdot 10^{-14}$ C. This value has been calculated from the known mass density $\rho = 1700 kg/m^3$ of the toner particles.

3. Results and Discussion

Numerical simulations with this model were found to give valuable insight into the role of collective effects of the charged toner particles. One of the problems that appeared during the development of the simulation program was, that the calculations did not agree with the experimental results. This was mainly caused by the neglect of space charge effects. It shall be remarked that the experiments were done with a conductive toner which is charged through induction. The amount of positive and negative charged toner particles is approximately the same, thus the total charge all particles together is nearly zero. Therefore, the charge cannot easily be measured with an electrometer. The above mentioned charge-to-mass ratio of the particles was determined in a Millikan experiment and applies as an average value for both polarities.

Although the total charge of the toner on the conveyor is nearly zero the assumption that no space charge is present would be misleading. When the simulations were calculated without any space charge field E_{space}, the particles always ended up in a curtain mode, even at very low frequencies. But in this mode the toner transport is much slower than it is observed experimentally. An analysis of the numerical results revealed that at low frequencies the particles do start in a synchronous mode but after some time all particles change into the much slower curtain mode. The reason for this is that under certain conditions the particles are repelled from the electrodes into very high regions where they can reach a stable position in the curtain mode. This observation clearly indicates that collective effects must be at work in the experiments that force the particles downwards and keep them moving in a faster mode near the conveyor surface.

But how can this happen when the total charge of the toner is almost zero? At least at low frequencies were a synchronous particle motion is predominant this is no contradiction, because the majority of particles are arranged in bands with the positive and negative charged particles being separated half a wavelength apart. For the asynchronous modes which appear at high frequencies the problem still remains unclear. It is not completely understood if strong space charge effects are at work or not.

For this reason only computations with unipolar positively charged particles are presented in this paper All calculations were done with these parameters:

- Toner conveyor: $L = 3$, $w/p = 0.56$
- Driving voltages: square wave, amplitude 350 V
- Space charge field: $E_{space,z} = -3 \cdot 10^5$ V/m

A snapshot of one simulation with a moderately low frequency of f = 500 Hz is shown in Fig. 6. Herein, the particles gather in bands that are spaced one wavelength apart which is characteristic for a synchronous motion. The particles move in a hopping manner with a speed near to the velocity $v_{fund} = \lambda \cdot f$ of the fundamental traveling electrostatic wave A similar behaviour is observed experimentally.

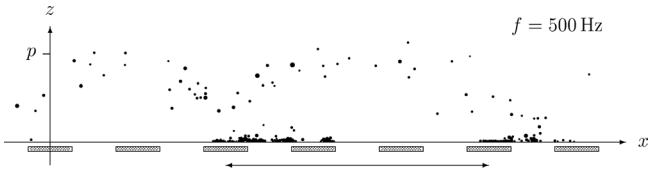

Figure 6. Snapshot of the simulated toner transport.

In general the simulations are in good agreement with the experiments over a wide range of frequencies as shown in Fig. 7 and Fig. 8. In the latter, the velocity of each individual particle is displayed as a small dot. These values were determined from the particle positions at 50 ms and 100 ms after the simulation started. In contrast to this, the experimental measurements where done with a high speed camera. Here the speed of the leading wave front of the traveling toner cloud was determined. Each of the large dots represents one measurement.

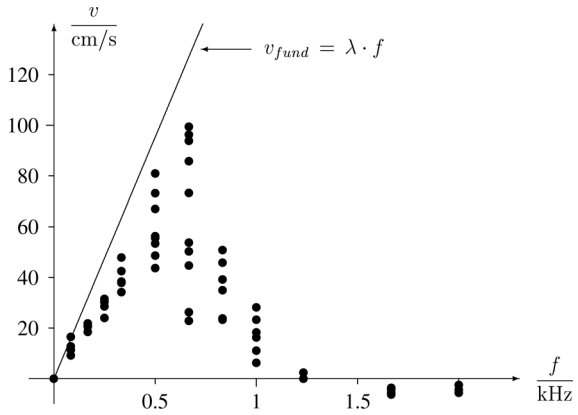

Figure 7. Experimentally measured velocity of the traveling toner

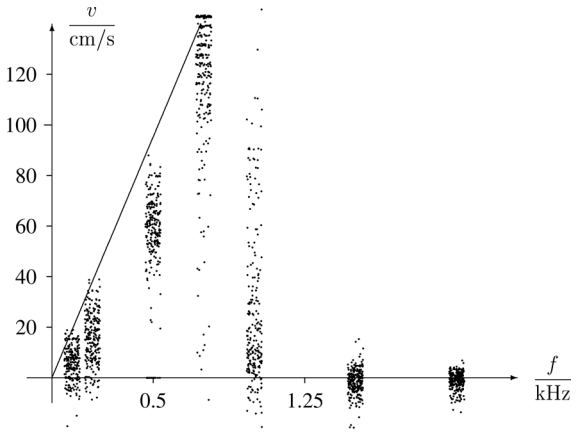

Figure 8. Numerically computed particle velocities

4. Conclusions

Numerical calculations can give valuable insight into the phenomenon of traveling wave toner transport. In realistic applications a large number of charged particles is present and therefore collective effects must be taken into account. Although the simulations in this paper are in good agreement with the experimental observations the space charge field in the model cannot be calculated exactly at present. Further research needs to be done for a better understanding of the importance of mutual interactions between traveling toner particles.

References

1. G. E. Keefe and E. J. Yarmchuk, Non-mechanical printing toner transport system, *IBM Tech. Discl. Bulletin*, **26**, 3450 (1983).
2. Fred W. Schmidlin, The role of traveling wave toner transport in powder printing, *Proc. IS&T's 11th Int. Congr. Adv. Non-Impact Print Technol.*, 515 (1995).
3. S. Masuda, K. Fajibayashi, K. Ishida, H. Inaba, Connement and transportation of charged aerosol clouds via electric curtain, *Elec. Eng. Japan*, **92**, 43 (1972).
4. J. R. Melcher, E. P. Warren and R. H. Kotwal, Theory for Pure-Traveling-Wave Boundary-Guided Transport of Tribo-Electried Particles, *Particulate Sci. Technol.*, **7**, 1 (1989).
5. J. R. Melcher, E. P. Warren and R. H. Kotwal, Theory for nitephase traveling-wave boundary-guided transport of triboelectri-ed particles, *IEEE Trans. Ind. Appl.*, **25**, 949 (1989).
6. Fred W. Schmidlin, A new nonlevitated mode of traveling wave toner transport, *IEEE Trans. Ind. Appl.*, **27**, 480 (1991).
7. D. Hu, W. Balachandran and W. Machowski, Computer user interface and simulation for designing a travelling wave panel electrode, *Conf. Rec. 1994 IAS Annual Meeting*, pg. 1621 (1994).
8. Fred W. Schmidlin, Modes of traveling wave particle transport and their applications, *J. Electrostatics*, **34**, 225 (1995).
9. W. Machowski and W. Balachandran, Electrodynamic control and separation of charged particles using travelling wave field technique, *J. Electrostatics*, 40-41, 325 (1997).
10. Fred W. Schmidlin, Advances in Traveling Wave Toner Transport, *Proc. NIP15: Int Conf Digital Print Technol.*, pg. 302 (1999).
11. Y. N. Gartstein and J. G. Shaw, Many-particle effects in traveling electrostatic wave transport, *J. Phys. D: Appl. Phys.*, **32**, 2176 (1999).
12. M. D. Thompson, Y. Gartstein and J. T. LeStrange, Aspects of Toner Transport on a Traveling Wave Device, *Proc. NIP15: Int. Conf. Digital Print Technol.*, pg 262 (1999).
13. J. G. Shaw and T. Retzlaff, Particle Simulation of Xerographic Development, *Proc. NIP12: Int. Conf. Digital Print Technol.*, pg 283 (1996).
14. J. G. Shaw and T. Retzlaff, Pseudoforce Based Computation of Charged Particle Dynamics, *Proc. 20th Annual Meeting Adhesion Soc.*, pg 223 (1996).
15. R. W. Hamming, *Numerical Methods for Scientists and Engineers*, Dover Publ., NY, 1986, pg 413.
16. R. Kober and B. Hill, An Experimental Setup for Bucket Brigade Toner Transport, *Proc. NIP15: Int. Conf. Digital Print Technol.*, pg 258 (1999).
17. R Kober, Traveling Wave Transport of Conductive Toner Particles, *Proc. NIP16: Int. Conf. Digital Print Technol*, pg 736 (2000).
18. G. Engeln-Muellges and Frank Uhlig, *Numerical Algorithms with C*, Springer, Berlin, 1996, pg 207.

Biography

Ralph Kober studied at the Aachen University of Technology and received his diploma in electrical engineering in 1995. His diploma thesis dealt with the experimental study of an electrostatic printing process with dry toner using an electronic printing plate. At present he is with the Technical Electronics Institute at the Aachen University of Technology. He is engaged in electrostatic printing technologies and traveling wave toner transport.